A New Spatio-Temporal Model for Random Access in Massive IoT Networks

Nan Jiang[*], Yansha Deng[*], Xin Kang[†], and Arumugam Nallanathan[‡]

[*]Department of Informatics, King's College London, London, UK
[†]National Key Laboratory of Science and Technology on Communications,
University of Electronic Science and Technology of China, China
[‡]School of Electronic Engineering and Computer Science, Queen Mary University of London, London, UK

Abstract—**Massive Internet of Things (mIoT) has provided an auspicious opportunity to build powerful and ubiquitous connections that faces a plethora of new challenges, where cellular networks are potential solutions due to their high scalability, reliability, and efficiency. The contention-based random access procedure (RACH) is the first step of connection establishment between IoT devices and Base Stations (BSs) in the cellular-based mIoT network, where modelling the interactions between static properties of physical layer network and dynamic properties of queue evolving in each IoT device are challenging. To tackle this, we provide a novel traffic-aware spatio-temporal model to analyze RACH in cellular-based mIoT networks, where the physical layer network are modelled and analyzed based on stochastic geometry, and the queue evolution are analyzed based on probability theory. For performance evaluation, we derive the exact expressions for the preamble transmission success probabilities of a randomly chosen IoT device with baseline scheme in each time slot. Our derived analytical results are verified by the realistic simulations capturing the evolution of packets in each IoT device.**

I. INTRODUCTION

Massive Internet of Things (mIoT) is deemed to connect billions of miscellaneous mobile devices or IoT devices, where a plethora of new applications, such as autonomous driving, smart-homes, and etc, are being innovated via mIoT. The successful operation of these IoT applications faces various challenges, among them providing wireless access for the tremendous number of IoT devices has been considered to be the main problem. According to the Third Generation Partnership Project (3GPP), the IoT technologies are suggested to be developed based on the existing cellular infrastructure, due to its zero additional hardware deployment cost as well as the high-level of security by operating on licensed band [1].

In the cellular-based mIoT network, a device performs random access channel procedure (RACH) when it needs to establish or re-establish a data connection with its associated BS, and the first step of RACH is that the device transmits a preamble via physical random access channel (PRACH). Generally, the contention-based RACH is much more sensitive to IoT traffic [2]. Most works on the analysis of contention-based RACH in cellular-based IoT networks, have only focused on addressing one of the following problems: 1) modelling packets success transmission impacted by physical channel propagation characteristics (e.g., the fading, noise and interference) [3]; 2) modelling time-varying queues and transmission schemes in MAC layer [4].

Stochastic geometry has been regarded as a powerful tool to model and analyze mutual interference between transceivers in the wireless networks, such as conventional cellular networks [5], wireless sensor networks [6], cognitive radio networks [7], device-to-device communication [8], and heterogenous cellular networks [9]. In these works, only the spatial distribution of transceivers is modelled, and the interactions between static properties of physical layer network and the dynamic properties of queue evolving in each transmitter are ignored due to the assumptions of backlogged network with saturated queues.

To model these aforementioned interactions, recent works have studied the stability of spatially spread interacting queues in the network based on stochastic geometry and queuing theory [10–12]. The work in [10] and [11] apply the stochastic geometry and queueing theory to analyze the performance of random access with each transmitter following a high mobility random walk and static, respectively. The work in [12] analyzed the delay in the heterogeneous cellular networks, and the statistics of such traffic with different offloading policies are compared.

In this paper, we develop a novel spatio-temporal mathematical framework for cellular-based mIoT network using stochastic geometry and probability theory, where the BSs and IoT devices are modelled as independent Poisson point processes (PPPs) in the spatial domain. In the time domain, the new arrival packets of each IoT device are modelled by independent Poisson arrival processes [12]. The contributions of this paper can be summarized in the following points:

- We present a novel spatio-temporal mathematical framework for analyzing RACH of cellular-based mIoT networks, where the packets accumulation and successful transmission of a typical IoT device in each time slot is accurately modelled. We derive the exact expression for the preamble transmission success probability of a randomly chosen IoT device in each time slot with the baseline scheme, where the queue statuses are firstly analyzed based on probability theory, and then approximated by their corresponding Poisson arrival distributions, which facilitates the queueing analysis.
- We develop a realistic simulation framework to capture the randomness location of IoT device, and the real packets arrival and success transmission of each IoT device in each time slot. Note that, the exact queueing

analysis is embedded into the simulation for the stochastic geometry analysis verification, the queue evolution as well as the stochastic geometry analysis are all verified by our proposed realistic simulation framework.

The rest of the paper is organized as follows. Section II presents the network model. Sections III derives preamble detection probability of a randomly chosen IoT device in each time slot with different schemes. Finally, Section IV concludes the paper.

II. SYSTEM MODEL

We consider an uplink model for cellular-based mIoT network consists of a single class of base stations (BSs) and IoT devices, which are spatially distributed in $\mathbb{R}^2$ following two independent homogeneous Poisson point process (PPP), Φ_B and Φ_D, with intensities λ_B and λ_D, respectively. Same as [5, 13], we assume each IoT device associates to its geographically closest BS, and thus forms a Voronoi tesselation, where the BSs are uniformly distributed in the Voronoi cell. Same as [11, 12, 14], the time is slotted into discrete time slots, and the number and locations of BSs and IoT devices are fixed all time once they are deployed.

A. Network Description

We consider a standard power-law path-loss model, where the signal power decays at a rate $r^{-\alpha}$ with the propagation distance r, and the path-loss exponent α. We consider Rayleigh fading channel, where the channel power gains $h(x, y)$ between two generic locations $x, y \in \mathbb{R}^2$ is assumed to be exponentially distributed random variables with unit mean. All the channel gains are independent of each other, independent of the spatial locations, and identically distributed (i.i.d.). For the brevity of exposition, the spatial indices (x, y) are dropped.

Uplink power control has been an essential technique in cellular network [5]. We assume that a full path-loss inversion power control is applied at all IoT devices, where each IoT device compensates for its own path-loss to keep the average received signal power equals to a same threshold ρ. The transmit power of ith IoT device P_i depends on the distance from its associated BS, and the defined threshold ρ, where $P_i = \rho r_i^\alpha$. Here, we assume that the density of BSs is high enough and none of the IoT device suffers from truncation outage.

B. Contention-Based Random Access Procedure

In LTE, the first step to establish an air interface connection is delivering requests to the associated BS via RACH, where the contention-based RACH is favored by mIoT network for the initial of uplink data transmission [15]. Contention-based RACH consists of 4 steps of data exchanging, and only the step 1 transmits signals via PRACH, but other steps transmit signals via normal uplink and downlink data transmission channel. Further details on the RACH can be found in [15]. In this paper, we only consider how preambles are transmitted via PRACH.

LTE defines prime-length Zadoff-Chu sequences as the random multiple access codes (also called preambles) for RACH, where different preambles are orthogonal [15]. In the mIoT network, each IoT device requests for access in the first available opportunity leading to a huge number of IoT devices transmit signals simultaneously, such that the network performance might degrade due to that the preambles cannot be detected or decoded by the BS [2]. This preamble transmission can be failed due to the following two reasons: 1) a signal cannot be recognized by the received BS, due to its low received SINR; 2) the BS successfully detected more than two signals using same preamble simultaneously, such that the collision occurs, and the BS cannot decode any collided signals. In this work, we limit ourselves to single preamble transmission fail, and leave the collision for our future work, thus we assume that a RACH procedure is always successful if the IoT device successfully transmits the preamble to its associated BS. Without loss of generality, we assume that each BS has an available preamble pool with same number of different preambles, known by its associated IoT devices, where N_p denotes the number of preambles. Each preamble has an equal probability $(1/N_p)$ to be chosen by an IoT device, and the average density of the IoT devices using the same preamble is $\lambda_{Dp} = \lambda_D/N_p$, where the λ_{Dp} is measured with unit devices/preamble/km^2.

C. Physical Random Access CHannel and Traffic Model

PRACHs is formed by sequences of allocated time-frequency resources, which are reserved in the uplink channel, and repeated in the system with a certain period that specified by the BS [2]. Without loss of generality, we assume that each time slot consists of a gap interval duration τ_g and a RACH duration τ_c, where the RACH duration τ_c is shorter than the gap interval duration τ_g as shown in the Fig. 1. We model the arrival of new packets in mth time slot at each IoT device as independent Poisson arrival process, Λ_{New}^m with same arrival rate $\varepsilon_{\text{New}}^m$ as [16]. It is assumed that the new packets arrival only takes place within the gap duration τ_g of each time slot, such that the number of new arrival packets N_{New}^m in duration τ_g is described by the Poisson distribution with $N_{\text{New}}^m\text{Pois}(\tau_g\varepsilon_{\text{New}}^m)$, where $\mu_{\text{New}}^m = \tau_g\varepsilon_{\text{New}}^m$. Within the duration of τ_g, the new arrival packets are stored in their buffers immediately, and then each device with non-empty buffer try to request uplink data transmission channel resources for its head-of-line packet in the following RACH within the duration of τ_c. Note that the data transmission after a successful RACH can be easily extended following the analysis of preamble transmission success probability in RACH. Due to the main focus of this paper is analyzing the time-slotted contention-based RACH in the mIoT network, we assume that the actual intended packet transmission is always successful if the corresponding RACH succeeds.

Each device is assumed to have an infinite buffer, where the arrived packets are stored in the buffer until successful transmission, and none of the packets will be dropped off. In each device, the packets are scheduled as a queue for

transmission, where each packet has same priority, and the BSs are unaware of the queue status of their associated IoT devices. Each IoT deivce transmits packets via a First Come First Serve (FCFS) packets scheduling scheme - the basic and the most simplest packet scheduling scheme, where all packets are treated equally by placing them at the end of the queue once they arrive [17].
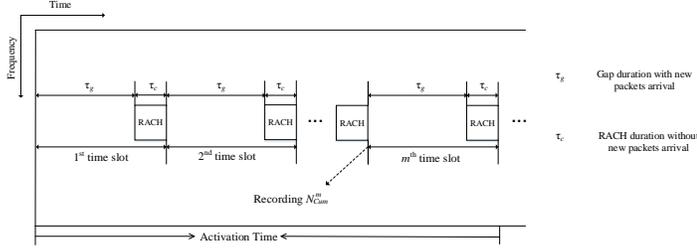

Fig. 1: RACH

TABLE I: The number of packets in buffer in each time slot.

Time Slot	Success	Failure
1st	$N_{Cum}^1 = 0$	$N_{Cum}^1 = 0$
2nd	$N_{Cum}^2 = N_{New}^1 - 1$	$N_{Cum}^2 = N_{New}^1$
3rd	$N_{Cum}^3 = N_{Cum}^2 + N_{New}^2 - 1$	$N_{Cum}^3 = N_{Cum}^2 + N_{New}^2$
$\vdots$	$\vdots$	$\vdots$
mth	$N_{Cum}^m = N_{Cum}^{m-1} + N_{New}^{m-1} - 1$	$N_{Cum}^m = N_{Cum}^{m-1} + N_{New}^{m-1}$

We consider basic transmission scheme - **baseline scheme** [18]: each IoT device transmits a packet when there exists packet in the buffer. The baseline scheme is the simplest scheme without any control of traffic. Due to the access request frequency is not be controlled at the IoT devices, the baseline scheme contributes to the fastest buffer flushing, such that it can provide a high data transmission rate with non-overloaded network condition. However, once the network is overloaded, high delays and service unavailability appear due to mass simultaneous access request.

In the temporal domain, the queue status of each device is evolved following transmission condition over time. A packet is removed from the buffer once it has been successfully transmitted to the BS, otherwise, this packet will be still in the first place of the queue, and the IoT device will try to request channel resources for the packet in the next available RACH. The number of accumulated packets in the buffer in mth time slot is denoted as N_{Cum}^m, where the buffer status N_{Cum}^m is recorded (Recording N_{Cum}^m in Fig.1) at the begin of the mth time slot. Note that the buffer of each IoT device is set empty at the beginning of the $1st$ time slot ($m = 1$). Evolving of queue status in an IoT device is described in Table I.

D. Signal to Noise plus Interference Ratio

A preamble can be successfully received at the associated BS, if its SINR is above the threshold. Based on Slivnyak's theorem [9], we formulate the SINR of a typical BS located at the origin as

$$SINR = \frac{\rho h_o}{\mathcal{I}_{\text{inter}} + \mathcal{I}_{\text{intra}} + \sigma^2}, \tag{1}$$

where ρ is full path-loss inversion power control threshold, h_o is channel power gain from the typical IoT device to its associated BS, σ^2 is noise power, $\mathcal{I}_{\text{inter}}$ is aggregate inter-cell interference, and $\mathcal{I}_{\text{intra}}$ is aggregate intra-cell interference. It is noted that only the non-empty IoT devices are active and generate interference, where the active probability of each IoT device can be treated using the thinning process. The active probability of each IoT device in the mth time slot $\mathcal{T}^m$ can be defined as

$$\mathcal{T}^m = \mathbb{P}\{N_{\text{New}}^m + N_{\text{Cum}}^m > 0\}, \tag{2}$$

where N_{New}^m is the number of new arrived packets in the mth time slot, and N_{Cum}^m is the number of accumulated packets in the mth time slot.

$$\mathcal{I}_{\text{intra}} = \sum_{j \in \mathcal{Z}_{in}} \mathbb{1}_{\{N_{\text{New}_j}^m + N_{\text{Cum}_j}^m > 0\}} \rho h_j, \tag{3}$$

where $\mathcal{Z}_{in}$ is the set of intra-cell interfering IoT devices, $\mathbb{1}_{\{\cdot\}}$ is the indicator function that takes the value 1 if the statement $\mathbb{1}_{\{\cdot\}}$ is true, and zero otherwise, $N_{\text{New}_j}^m$ is the number of new arrived packets of jth device in the mth time slot, $N_{\text{Cum}_j}^m$ is the number of accumulated packets of jth device in the buffer in the mth time slot, h_j is channel power gain from the jth intra-cell interfering IoT device to the typical BS. The aggregate inter-cell interference is expressed as

$$\mathcal{I}_{\text{inter}} = \sum_{u_i \in \mathcal{Z}_{out}} \mathbb{1}_{\{N_{\text{New}_i}^m + N_{\text{Cum}_i}^m > 0\}} P_i h_i \|u_i\|^{-\alpha}, \tag{4}$$

where $\mathcal{Z}_{out}$ is the set of inter-cell interfering IoT devices, $\|\cdot\|$ is the Euclidean norm, $N_{\text{New}_i}^m$ is the number of new arrived packets of ith device in the mth time slot, $N_{\text{Cum}_i}^m$ is the number of accumulated packets of ith device in the buffer in the mth time slot, h_i is channel power gain from the ith inter-cell interfering IoT device to the typical BS, u_i is the distance between the ith inter-cell IoT device and the typical BS, and P_i is the actual transmit power of the ith inter-cell IoT device, and P_i depends on the power control threshold ρ and the distance between the ith inter-cell typical IoT device and its associated BS r_i with $P_i = \rho r_i^\alpha$.

III. ANALYSIS UNDER THE PROPOSED SPATIO-TEMPORAL MODEL

A. Stochastic Geometry Model

In this section, we first analyze the stochastic geometry model in the spatial domain. Note that inactive IoT devices (those with no packet in buffer) do not request to access to its associated BS, such that they do not generating interference. Due to that the preamble (sub-channel) has an equal probability to be chosen, the analysis performed on a randomly chosen preamble can represent the whole network. The probability that the received SINR at BS exceeds γ_{th} is written as

$$\mathbb{P}\left\{\frac{\rho h_o}{\mathcal{I}_{\text{inter}} + \mathcal{I}_{\text{intra}} + \sigma^2} \geq \gamma_{\text{th}}\right\}$$
$$= \exp\left(\frac{\gamma_{\text{th}}}{\rho}\sigma^2\right) \mathcal{L}_{\mathcal{I}_{\text{intra}}}\left(\frac{\gamma_{\text{th}}}{\rho}\right) \mathcal{L}_{\mathcal{I}_{\text{inter}}}\left(\frac{\gamma_{\text{th}}}{\rho}\right), \tag{5}$$

where $\mathcal{L}_{\mathcal{I}}(\cdot)$ denotes the Laplace Transform of the PDF of the aggregate interference $\mathcal{I}$. Note that whether an IoT device is

active only depends on the new packets arrival process Λ^1_{New} in the 1st time slot, such that the active probability of each IoT device $\mathcal{T}^1$ in the 1st time slot is expressed as

$$\mathcal{T}^1 = \mathbb{P}\left\{N^1_{\mathrm{New}} > 0\right\} = 1 - e^{-\mu^1_{\mathrm{New}}}, \qquad (6)$$

where $\mu^1_{\mathrm{New}} = \tau_g \varepsilon^1_{\mathrm{New}}$, $\varepsilon^1_{\mathrm{New}}$ is the new packets arrival rate of each IoT device in the 1st time slot, and the probability that no packet arrives ($N^1_{\mathrm{New}} = 0$) during τ_g in the 1st time slot is equal to $e^{-\tau_g \mu^1_{\mathrm{New}}}$.

We perform the analysis on a BS associating with a randomly chosen IoT device, where the other active IoT devices choosing same preamble are visualized as interfering IoT devices. The Laplace Transform of aggregate inter-cell interference is characterized in the following Lemma.

Lemma 1. *The LT of aggregate inter-cell interference received at the typical BS in the cellular-based mIoT network is given by*

$$\mathcal{L}_{\mathcal{I}_{\mathrm{inter}}}(\frac{\gamma_{\mathrm{th}}}{\rho}) = \exp\left(-2(\gamma_{\mathrm{th}})^{\frac{2}{\alpha}} \frac{\mathcal{T}^1 \lambda_{Dp}}{\lambda_B} \int_{(\gamma_{\mathrm{th}})^{\frac{-1}{\alpha}}}^{\infty} \frac{y}{1+y^\alpha} dy\right), \quad (7)$$

where $\mathcal{T}^1$ is the active probability of each IoT devices being given in (6). Remind that λ_{Dp} is the intensity of IoT devices using same preamble.

Proof. See Appendix A. □

Since the interference generating by each intra-cell IoT device is strictly equal to ρ, such that the aggregate intra-cell interference only depends on the number of active interfering IoT devices in the Voronoi cell. We assume $\widehat{Z}_{in}$ denotes the number of active IoT device in a specific Voronoi cell, and let $Z_D = \left|\widehat{Z}_{in}\right| - 1$ denotes the number of active interfering IoT devices in such cell, where the Laplace Transform of aggregate intra-cell interference is conditioned on Z_D. The Probability Density Function (PDF) of the number of active interfering IoT devices in a Voronoi cell has been derived by the Monte Carlo method in [19], and the Probability Mass function (PMF) of the number of interfering IoT devices Z_D in a BS with a randomly chosen IoT device has been clearly introduced in [20], which is expressed as

$$\mathbb{P}\{Z_D = n\} = \frac{c^{(c+1)}\Gamma(n+c+1)(\frac{\mathcal{T}^1 \lambda_{Dp}}{\lambda_B})^n}{\Gamma(c+1)\Gamma(n+1)(\frac{\mathcal{T}^1 \lambda_{Dp}}{\lambda_B}+c)^{n+c+1}}. \qquad (8)$$

Lemma 2. *The Laplace Transform of aggregate intra-cell interference at the BS to which a randomly chosen IoT device belongs in the cellular-based mIoT network is given by*

$$\mathcal{L}_{\mathcal{I}_{\mathrm{intra}}}(\frac{\gamma_{\mathrm{th}}}{\rho}) = \left(1 + \frac{\mathcal{T}^1 \lambda_{Dp} \gamma_{\mathrm{th}}}{c\lambda_B(1+\gamma_{\mathrm{th}})}\right)^{-c-1}, \qquad (9)$$

where $c = 3.575$ is a constant related to the approximate PMF of the PPP Voronoi cell, and $\Gamma(\cdot)$ is gamma function.

Proof. See Appendix B. □

Substituting (7) and (9) into (5), we derive the preamble transmission success probability of the 1st time slot P^1_t in the following theorem.

Theorem 1. *In the depicted cellular-based mIoT network, the preamble transmission success probability of a randomly chosen IoT device of the 1st time slot is given by*

$$\mathcal{P}^1_t = \exp\left(-\frac{\gamma_{\mathrm{th}}\sigma^2}{\rho} - 2(\gamma_{\mathrm{th}})^{\frac{2}{\alpha}} \frac{\mathcal{T}^1 \lambda_{Dp}}{\lambda_B} \int_{(\gamma_{\mathrm{th}})^{\frac{-1}{\alpha}}}^{\infty} \frac{y}{1+y^\alpha} dy\right)$$
$$\left(1 + \frac{\mathcal{T}^1 \lambda_{Dp} \gamma_{\mathrm{th}}}{c\lambda_B(1+\gamma_{\mathrm{th}})}\right)^{-c-1}. \qquad (10)$$

Proof. The proof follows from Theorem 1. □

In Theorem 1, the preamble transmission success probability at a *randomly chosen IoT device* is described by the number of interfering intra-cell IoT devices in that cell, where that randomly chosen IoT device belongs to in (8).

B. Queue Evolution Model

Next, we analyze the performance of the cellular-based mIoT network in each time slot with the baseline scheme. We first introduce how to analyze the queue evolution.

We start by studying the preamble transmission success probability of the baseline scheme at any time slot. The queue status and the preamble transmission success probability are interdependent, and imposes a causality problem. More specifically, the preamble transmission success probability of current time slot depends on the aggregate interference from those active IoT devices with packets in their buffer in that time slot, thus we need to know the current queue status, which is decided by the previous queue statuses, as well as the preamble transmission success probabilities of previous time slots. Recall that the evolution of queue status follows Table I, where the accumulated packets come from the packets that are not successfully transmitted in the previous time slots. Next, we provide two approaches to derive the PMF and CDF of the N^m_{Cum} of each time slot, which are probabilistic statistics and Poisson approximation.

1) Probabilistic Statistics: The PMF of the cumulated packets in the 2nd time slot N^2_{Cum} is expressed as

$$f_{N^2_{\mathrm{Cum}}}(x) = \begin{cases} e^{-\mu^1_{\mathrm{New}}} + \mu^1_{\mathrm{New}} e^{-\mu^1_{\mathrm{New}}} \mathcal{P}^1_t, & x = 0, \\ \dfrac{(\mu^1_{\mathrm{New}})^x e^{-\mu^1_{\mathrm{New}}}}{x!}(1 - \mathcal{P}^1_t) + \\ \dfrac{(\mu^1_{\mathrm{New}})^{x+1} e^{-\mu^1_{\mathrm{New}}}}{(x+1)!} \mathcal{P}^1_t, & x > 0, \end{cases} \qquad (11)$$

where $\mu^1_{\mathrm{New}} = \tau_g \varepsilon^1_{\mathrm{New}}$, $\varepsilon^1_{\mathrm{New}}$ is the new packets arrival rate of each IoT device in the 1st time slot, and P^1_t is the preamble transmission success probability of the IoT device in the 1st time slot given in (10). The reason for (11) is the number of cumulated packets in the 2nd time slot equals to x occurs only when 1) the number of cumulated packets in the 1st time slot equals to $x+1$, and one packet is successfully transmitted in the 1st time slot, and 2) the number of cumulated packets in the 1st time slot equals to x, and no packet is successfully transmitted in the 1st time slot.

Based on (11), we derive the CDF of the number of cumulated packets in the 2nd time slot N^2_{Cum} as

$$F_{N^2_{\text{Cum}}}(y) = \sum_{x=0}^{y}\left(\frac{(\mu^1_{\text{New}})^x e^{-\mu^1_{\text{New}}}}{x!}\right) + \frac{(\mu^1_{\text{New}})^{y+1} e^{-\mu^1_{\text{New}}}}{(y+1)!}\mathcal{P}^1_t. \quad (12)$$

We are interested in the zero-cumulated packets probability in the 2nd time slot, since it determines the density of active IoT devices (with more than one packet in the buffer) in that time slot, and the activity probability of IoT devices. Based on the probabilistic statistics and (11), we present the active probability of IoT devices in the $2nd$ time slot as

$$\mathcal{T}^2 = \left(1 - e^{-\mu^2_{\text{New}}}\right)\left(e^{-\mu^1_{\text{New}}} + \mu^1_{\text{New}} e^{-\mu^1_{\text{New}}}\mathcal{P}^1_t\right). \quad (13)$$

Following the proof of Theorem 2 and substituting (13) into (A.1), we derive the preamble transmission success probability of a randomly chosen IoT device in the 2nd time slot as

$$\mathcal{P}^2_t = \exp\left(-\frac{\gamma_{\text{th}}\sigma^2}{\rho} - 2(\gamma_{\text{th}})^{\frac{2}{\alpha}}\frac{\mathcal{T}^2\lambda_{Dp}}{\lambda_B}\int_{(\gamma_{\text{th}})^{\frac{-1}{\alpha}}}^{\infty}\frac{y}{1+y^\alpha}dy\right)$$
$$\left(1 + \frac{\mathcal{T}^2\lambda_{Dp}\gamma_{\text{th}}}{c\lambda_B(1+\gamma_{\text{th}})}\right)^{-c-1}. \quad (14)$$

Similar as (11) and (12), we can derive the PMF and the CDF of the number of cumulated packets in the 3rd time slot N^3_{Cum} as

$$f_{N^3_{\text{Cum}}}(x) =$$
$$\begin{cases} e^{-\mu^2_{\text{New}}}f_{N^2_{\text{Cum}}}(0) + \\ \mathcal{P}^2_t\left[\mu^2_n e^{-\mu^2_{\text{New}}}f_{N^2_{\text{Cum}}}(0) + e^{-\mu^2_{\text{New}}}f_{N^2_{\text{Cum}}}(1)\right], & x = 0, \\ (1-\mathcal{P}^2_t)\sum_{z=0}^{x}\left[\frac{(\mu^1_{\text{New}})^z e^{-\mu^1_{\text{New}}}}{(z)!}f_{N^2_{\text{Cum}}}(x-z)\right] + \\ \mathcal{P}^2_t\sum_{z=0}^{x+1}\left[\frac{(\mu^1_{\text{New}})^z e^{-\mu^1_{\text{New}}}}{(z)!}f_{N^2_{\text{Cum}}}(x-z)\right], & x > 0, \end{cases} \quad (15)$$

and

$$F_{N^3_{\text{Cum}}}(y) = \sum_{x=0}^{y}\sum_{z=0}^{x}\left[\frac{(\mu^1_{\text{New}})^z e^{-\mu^1_{\text{New}}}}{(z)!}f_{N^2_{\text{Cum}}}(x-z)\right] +$$
$$\mathcal{P}^2_t\sum_{z=0}^{y+1}\left[\frac{(\mu^1_{\text{New}})^z e^{-\mu^1_{\text{New}}}}{(z)!}f_{N^2_{\text{Cum}}}(y-z)\right], \quad (16)$$

respectively. In (15) and (16), $f_{N^2_{\text{Cum}}}(x)$ is given in (11), and $\mathcal{P}^2_t$ is given in (14). The PMF and CDF of N^m_{Cum} in the mth time slot can be calculated by the iteration process, however, as m increases, it becomes more complicated, and hard to analysis. As such, we approximate the number of cumulated packets in the mth time slot as a Poisson distribution ($m > 1$) in the following subsection, which largely simplifies the derivations.

2) Poisson Approximation: We approximate the number of accumulated packets of an IoT device in mth time slot N^m_{Cum} as Poisson distribution Λ^m_{Cum} with intensity μ^m_{Cum}. The intensity of the accumulated packets in the 1st time slot μ^1_{Cum} is equal to zero, due to the buffer of each IoT device is set as empty at the beginning of the first time slot ($N^1_b = 0$). In the 2nd time slot, μ^2_{Cum} depends on the new packets arrival rate

μ^1_{New} and the preamble transmission success probability P^1_t of an IoT device in the 1st time slot, which is given by

$$\mu^2_{\text{Cum}} = \mathcal{P}^1_t\left(\underbrace{\sum_{x=1}^{\infty}f_{N^1_{\text{Cum}}}(x)\cdot(x-1)}_{(a)}\right) + \left(1-\mathcal{P}^1_t\right)\left(\underbrace{\sum_{x=1}^{\infty}f_{N^1_{\text{Cum}}}(x)\cdot x}_{(b)}\right)$$
$$= \mathcal{P}^1_t\left(\sum_{x=1}^{\infty}\frac{(\mu^1_{\text{New}})^x e^{-\mu^1_{\text{New}}}(x-1)}{x!}\right) + \left(1-\mathcal{P}^1_t\right)\mu^1_{New}$$
$$= \mathcal{P}^1_t\left(\sum_{x=0}^{\infty}\frac{(\mu^1_{\text{New}})^x e^{-\mu^1_{\text{New}}}x}{x!} - \sum_{x=1}^{\infty}\frac{(\mu^1_{New})^x e^{-\mu^1_{New}}}{x!}\right)$$
$$+ \left(1-\mathcal{P}^1_t\right)\mu^1_{New}$$
$$= \mu^1_{New} - \mathcal{P}^1_t\left(1 - e^{-\mu^1_{New}}\right), \quad (17)$$

where $\mu^1_n = \tau_g \varepsilon^1_n$, ε^1_n is the new packets arrival rate of each device in the 1st time slot, $f_{N^1_{Cum}}(\cdot)$ is the PMF of the number of new arrived packets N^1_{Cum}, P^1_t is given in (10) of Theorem 1. In (17), (a) is the density of the cumulated packets in the 2nd time slot due to the success transmission in the 1st time slot, and (b) is the density of the cumulated packets in the 2nd time slot due to the unsuccess transmission in the 1st time slot.

According to Poisson approximation and (17), the CDF of the number of packets in the 2nd time slot due to previous cumulated packets N^2_{Cum} is approximated as

$$F_{N^2_{Cum}}(y) \approx \sum_{z=0}^{y}\frac{1}{z!}\left(\mu^2_{Cum}\right)^z e^{-\mu^2_{Cum}}$$
$$= \sum_{z=0}^{y}\frac{1}{z!}\left(\mu^1_{New} - \mathcal{P}^1_t\left(1-e^{-\mu^1_{New}}\right)\right)^z e^{-\mu^1_{New}-\mathcal{P}^1_t\left(1-e^{-\mu^1_{New}}\right)}, \quad (18)$$

and the active probability of an IoT devices in the 2nd time slot is approximated as

$$\mathcal{T}^2 \approx 1 - e^{-\mu^2_{New}-\mu^2_{Cum}}, \quad (19)$$

where μ^2_{New} is given in (17).

Similarly, the intensity of the number of accumulated packets in the 3rd time slot μ^3_{Cum} is

$$\mu^3_{Cum} = \mu^2_{New} + \mu^2_{Cum} - \mathcal{P}^2_t\left(1 - e^{-\mu^2_{New}-\mu^2_{Cum}}\right), \quad (20)$$

where μ^2_{Cum} is given in (17), and $\mathcal{P}^2_t$ is given in (14). Thus, we approximate the CDF of the number of accumulated packets in the 3nd time slot N^3_{Cum} as

$$F_{N^3_{Cum}}(y) \approx \sum_{z=0}^{y}\frac{(\mu^3_{Cum})^z e^{-\mu^3_{Cum}}}{z!}, \quad (21)$$

where μ^3_{Cum} is given in (20). The active probability of an IoT device in the 3rd time slot $\mathcal{T}^3$ under the Poisson approximation is expressed as

$$\mathcal{T}^3 \approx 1 - e^{-\mu^3_{New}-\mu^3_{Cum}}. \quad (22)$$

Fig. 2 shows the CDFs of the number of accumulated packets via simulation, as well as calculating by the probabilistic statistics and the Poisson approximation. We see the close match among the probabilistic statistics, Poisson approximation and the simulation results, which validates our approximation approach.

Based on the iteration process, we can derive the active probability of an IoT device in the mth time slot, and then derive the preamble transmission success probability of an IoT device in the mth time slot. The preamble transmission success probability of a randomly chosen IoT device in mth time slot in the following Theorem.
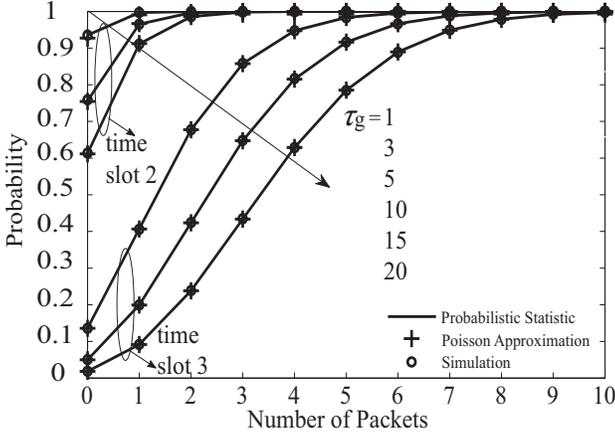

Fig. 2: Comparing the CDFs of the number of accumulated packets between probabilistic statistics and Poisson approximation in 2nd and 3rd. The simulation parameters are $\lambda_B = 10$ BS/km^2, $\lambda_{Dp} = 100$ IoT deivces/preamble/km^2, $\rho = -90$ dBm, $\sigma^2 = -90$ dBm, and $\varepsilon_{New}^1 = \varepsilon_{New}^2 = \varepsilon_{New}^3 = 0.1$ packets/ms.

Theorem 2. *The preamble transmission success probability of a randomly chosen IoT device in the mth time slot in the spatio-temporal model is derived as*

$$\mathcal{P}_t^m = \exp\left(-\frac{\gamma_{\text{th}}\sigma^2}{\rho} - 2(\gamma_{th})^{\frac{2}{\alpha}}\frac{\mathcal{T}^m\lambda_{Dp}}{\lambda_B}\int_{(\gamma_{th})^{\frac{-1}{\alpha}}}^{\infty}\frac{y}{1+y^\alpha}dy\right)$$
$$\left(1+\frac{\mathcal{T}^m\lambda_{Dp}\gamma_{th}}{c\lambda_B(1+\gamma_{th})}\right)^{-c-1}, \qquad (23)$$

where the active probability of each IoT device is
$$\mathcal{T}^m = 1 - e^{-\mu_{New}^m - \mu_{Cum}^m}, \qquad (24)$$

where the intensity of number of accumulated packets μ_{Cum}^m is

$$\mu_{Cum}^m = \begin{cases} 0, & m=1, \\ \mu_{New}^{m-1} - \mathcal{P}_t^{m-1}\left(1-e^{-\mu_{New}^{m-1}}\right), & m=2, \\ \mu_{New}^{m-1} + \mu_{Cum}^{m-1} & \\ \quad - \mathcal{P}_t^{m-1}\left(1-e^{-\mu_{New}^{m-1}-\mu_{Cum}^{m-1}}\right), & m>2. \end{cases} \qquad (25)$$

IV. NUMERICAL RESULTS

In this section, we validate our analysis via independent system level simulations, where the BSs and IoT devices are deployed via independent PPPs in a 100 km^2 area. Each IoT device employs the channel inversion power control, and associated with its nearest BS. Importantly, the real buffer at each IoT device is simulated to capture the packets arrival and accumulation process evolved along the time. The received SINR of each active IoT device in each time slot is captured, and compared with the SINR threshold γ_{th} to determine the success or failure of each RACH attempt. Unless otherwise stated, we set the same new packets arrival rate for each time slot ($\varepsilon_{\text{New}}^1 = \varepsilon_{\text{New}}^2 = \varepsilon_{\text{New}}^3 = \cdots = \varepsilon_{\text{New}}^m = 0.1$ packets/ms),

$\rho = -90$ dBm, $\sigma^2 = -90$ dBm, $\lambda_B = 10$ BS/km^2, $\lambda_{Dp} = 100$ IoT deivces/preamble/km^2, $\alpha = 4$, and $\gamma_{\text{th}} = -10$ dB.

Fig. 3 plots the preamble transmission success probability $\mathcal{P}_t^1$ versus the SINR threshold (γ_{th}) for the 1st single time slot. We set the duration of gap interval between two RACHs as $\tau_g = 1$ ms, which is the duration of gap interval between two RACHs, and $\mu_{New}^1 = \tau_g \cdot \varepsilon_{New}^1 = 0.1$. The analytical curves of the preamble transmission success probability are plotted using (10). We first see the well match between the analysis and the simulation results, which validates the accuracy of developed single time slot mathematical framework. As expected, the preamble transmission success probability increases with decreasing the SINR threshold.
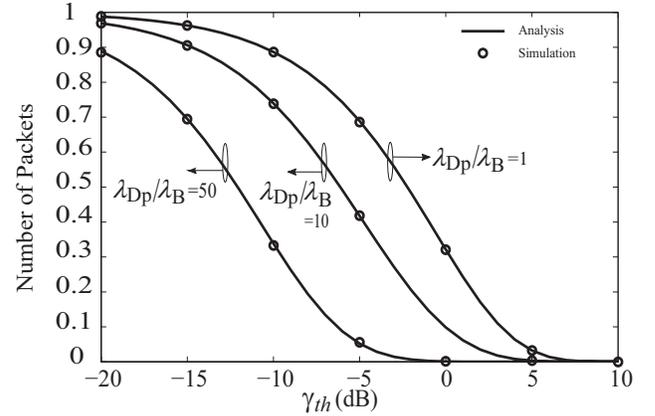

Fig. 3: Preamble transmission success probability for the single 1st time slot.
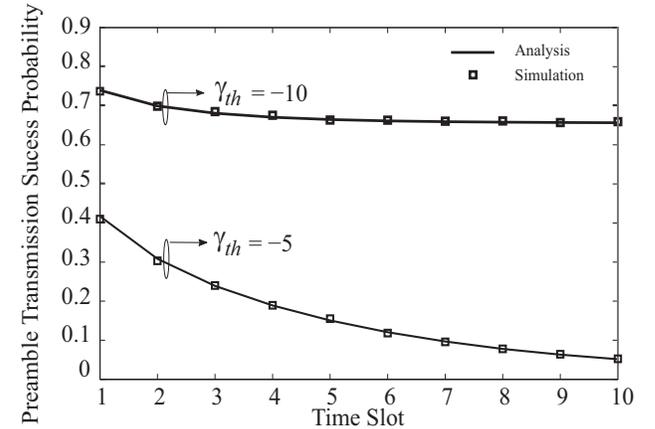

Fig. 4: Preamble transmission success probability for the multiple time slots.

Fig. 4 plots the preamble transmission success probabilities of a random IoT device at each time slot with the baseline scheme. The preamble transmission success probabilities decrease with increasing time, due to that the intensity of interfering IoT devices grows with increasing active probability of each IoT device, caused by the increasing average number of accumulated packets. Its preamble transmission success probability with $\gamma_{th} = -5$ dB decreases faster than that with $\gamma_{th} = -10$ dB, due to the higher chance of the accumulated

packets being reduced for $\gamma_{th} = -10$ dB leading to relatively lower average active probability of each IoT device.

V. Conclusion

In this paper, we developed a spatio-temporal mathematical model to analyze the RACH of cellular-based mIoT networks. We derived the preamble transmission success probabilities of a randomly chosen IoT device with the baseline scheme by modelling the queue evolution over different time slot. Our numerical results showed that the baseline scheme with low SINR threshold outperforms that with high SINR threshold, and such gap increases with increasing time. The analytical model presented in this paper can also be applied for the performance evaluation of other types of RACH transmission schemes in the cellular-based networks by substituting its packets evolution principle.

Appendix A
A Proof of Lemma 1

The Laplace Transform of aggregate inter-cell interference can be derived as

$$
\mathcal{L}_{I_{inter}}(s) \overset{(a)}{=} E_{\widehat{Z}_{out}} \Big[\prod_{u_i \in \widehat{Z}_{out}} E_{P_i} E_{h_i} \Big[e^{-sP_i h_i \|u_i\|^{-\alpha}} \Big] \Big]
$$

$$
\overset{(b)}{=} \exp \left(-2\pi \mathcal{T}^1 \lambda_{Dp} \int_{(P/\rho)^{\frac{1}{\alpha}}}^{\infty} E_P E_h \left[1 - e^{-sPhx^{-\alpha}} \right] x dx \right)
$$

$$
\overset{(c)}{=} \exp \left(-2\pi \mathcal{T}^1 \lambda_{Dp} s^{\frac{2}{\alpha}} E_P[P^{\frac{2}{\alpha}}] \int_{(s\rho)^{\frac{-1}{\alpha}}}^{\infty} \frac{y}{1 + y^\alpha} dy \right), \quad (A.1)
$$

where $s = \gamma_{th}/\rho$, $E_x[*]$ is the expectation with respect to the random variable x, $\mathcal{T}^1$ is the active probability of each IoT devices being given in (6), (a) follows from independence between λ_{Dp}, P_i, and h_i, (b) follows from the probability generation functional (PGFL) of the PPP, and (c) obtained by changing the variables $y = \frac{x}{(SP)^{\frac{1}{\eta}}}$. The kth moments of the transmit power is expressed as [13]

$$
E_P[P^k] = \frac{\rho^k \gamma\left(\frac{k\alpha}{2} + 1, \pi \lambda_B \left(\frac{P}{\rho} \right)^{\frac{2}{\alpha}} \right)}{(\pi \lambda_B)^{\frac{k\alpha}{2}} \left(1 - e^{-\pi \lambda_B \left(\frac{P}{\rho} \right)^{\frac{2}{\alpha}}} \right)}, \quad (A.2)
$$

where $\gamma(a, b) = \int_0^b t^{a-1} e^{-t} dt$ is the lower incomplete gamma function. Substituting (A.2) into (A.1), we derive the Laplace Transform of aggregate inter-cell interference.

Appendix B
A Proof of Lemma 2

The Laplace Transform of aggregate intra-cell interference is conditioned on known the number of interfering intra-cell IoT devices Z_D given as

$$
\mathcal{L}_{\mathcal{I}_{intra}}(s) = \sum_{n=0}^{\infty} \mathbb{P}\{Z_B = n\} \left(E\left[e^{-sI} \right] \big| Z_D = n \right)
$$

$$
= \mathbb{P}\{Z_D = 0\} + \sum_{n=1}^{\infty} \mathbb{P}\{Z_D = n\} E_{h_n} \left[\exp \left(-s \sum_{1}^{n} \rho h_n \right) \right]
$$

$$
\overset{(a)}{=} \mathbb{P}\{Z_D = 0\} + \sum_{n=1}^{\infty} \mathbb{P}\{Z_D = n\} \left(\frac{1}{1 + s\rho} \right)^n, \quad (B.1)
$$

where $s = \gamma_{\text{th}}/\rho$, $\mathbb{P}\{Z_D = n\}$ is the probability of the number of interfering intra-cell IoT devices $Z_D = n$ given in (8), and (a) follows from the Laplace Transform of h_n. After some mathematical manipulations, we proved (9) in Lemma 2.

References

[1] Ericsson. Cellular networks for massive IoT - enabling low power wide area applications. *White Paper*, 2016.

[2] Andres Laya, Luis Alonso, and Jesus Alonso-Zarate. Is the random access channel of LTE and LTE-A suitable for M2M communications? a survey of alternatives. *IEEE Commun. Surveys Tuts.*, 16(1):4–16, Jan. 2014.

[3] François Baccelli, Bartłomiej Błaszczyszyn, and Paul Mühlethaler. Stochastic analysis of spatial and opportunistic aloha. *IEEE J. Sel. Areas Commun.*, 27(7):1105–1119, Sep. 2009.

[4] Israel Leyva-Mayorga, Luis Tello-Oquendo, Vicent Pla, Jorge Martinez-Bauset, and Vicente Casares-Giner. Performance analysis of access class barring for handling massive M2M traffic in LTE-A networks. In *Int. Conf. Commun. (ICC)*, pages 1–6. IEEE, 2016.

[5] Thomas D Novlan, Harpreet S Dhillon, and Jeffrey G Andrews. Analytical modeling of uplink cellular networks. *IEEE Trans. Wireless Commun.*, 12(6):2669–2679, Jun. 2013.

[6] Yansha Deng, Lifeng Wang, Maged Elkashlan, Arumugam Nallanathan, and Ranjan K Mallik. Physical layer security in three-tier wireless sensor networks: A stochastic geometry approach. *IEEE Trans. Inf. Forensics Security*, 11(6):1128–1138, Jun. 2016.

[7] Yansha Deng, Lifeng Wang, Syed Ali Raza Zaidi, Jinhong Yuan, and Maged Elkashlan. Artificial-noise aided secure transmission in large scale spectrum sharing networks. *IEEE Trans. Commun.*, 64(5):2116–2129, May. 2016.

[8] Mansour Naslcheraghi, Seyed Ali Ghorashi, and Mohammad Shikh-Bahaei. Performance analysis of inband fd-d2d communications with imperfect si cancellation for wireless video distribution. *arXiv preprint arXiv:1706.06142*, 2017.

[9] Yansha Deng, Lifeng Wang, Maged Elkashlan, Marco Di Renzo, and Jinhong Yuan. Modeling and analysis of wireless power transfer in heterogeneous cellular networks. *IEEE Trans. Commun.*, 64(12):5290–5303, Dec. 2016.

[10] Kostas Stamatiou and Martin Haenggi. Random-access poisson networks: stability and delay. *IEEE Commun. Lett.*, 14(11):1035–1037, Nov. 2010.

[11] Yi Zhong, Martin Haenggi, Tony QS Quek, and Wenyi Zhang. On the stability of static poisson networks under random access. *IEEE Trans. Commun.*, 64(7):2985–2998, Jul. 2016.

[12] Yi Zhong, Tony QS Quek, and Xiaohu Ge. Heterogeneous cellular networks with spatio-temporal traffic: Delay analysis and scheduling. *arXiv preprint arXiv:1611.08067*, 2016.

[13] H. ElSawy and E. Hossain. On stochastic geometry modeling of cellular uplink transmission with truncated channel inversion power control. *IEEE Trans. Wireless Commun.*, 13(8):4454–4469, Aug. 2014.

[14] Nan Jiang, Yansha Deng, Xin Kang, and Arumugam Nallanathan. Random access analysis for massive iot networks under a new spatio-temporal model: A stochastic geometry approach. *arXiv preprint arXiv:1704.01988*, 2017.

[15] Erik Dahlman, Stefan Parkvall, and Johan Skold. *4G: LTE/LTE-advanced for mobile broadband*. Academic press, 2013.

[16] Kaijie Zhou, Navid Nikaein, and Thrasyvoulos Spyropoulos. LTE/LTE-A discontinuous reception modeling for machine type communications. *IEEE Commun. Lett.*, 2(1):102–105, Feb. 2013.

[17] Gordon Gow and Richard Smith. *Mobile and wireless communications: an introduction*. McGraw-Hill Education (UK), 2006.

[18] Study on RAN improvements for machine-type communications. *3GPP, Sophia, Antipolis, France, TR 37.868 V11.0.0,*, Sep. 2011.

[19] Járai-Szabó Ferenc and Zoltán Néda. On the size distribution of poisson voronoi cells. *Phys. A: Statistical mech. appl.*, 385(2):518–526, Nov. 2007.

[20] S. M. Yu and S. L. Kim. Downlink capacity and base station density in cellular networks. In *Proc. Int. Symp. Modeling Mobile Ad Hoc WiOpt Netw.*, pages 119–124, May. 2013.